



# EPA Public Access

Author manuscript

*Sci Total Environ.* Author manuscript; available in PMC 2019 February 15.

About author manuscripts

Submit a manuscript

Published in final edited form as:

*Sci Total Environ.* 2018 February 15; 615: 150–160. doi:10.1016/j.scitotenv.2017.09.033.

## High-throughput in-silico prediction of ionization equilibria for pharmacokinetic modeling

Cory L. Strope<sup>a,b,e,\*</sup>, Kamel Mansouri<sup>b,f</sup>, Harvey J. Clewell III<sup>f</sup>, James R. Rabinowitz<sup>c</sup>, Caroline Stevens<sup>d</sup>, and John F. Wambaugh<sup>c</sup>

<sup>a</sup>Risk Assessment Division, Office of Pollution Prevention and Toxics, Office of Chemical Safety and Pollution Prevention, U.S. Environmental Protection Agency, Washington, DC, USA

<sup>b</sup>ORISE Postdoctoral Research Fellow, National Center for Computational Toxicology, Office of Research and Development, U.S. Environmental Protection Agency, Research Triangle Park, NC, USA

<sup>c</sup>National Center for Computational Toxicology, Office of Research and Development, U.S. Environmental Protection Agency, Research Triangle Park, NC, USA

<sup>d</sup>Ecosystems Research Division, National Exposure Research Laboratory, Office of Research and Development, U.S. Environmental Protection Agency, Athens, GA, USA

<sup>e</sup>The Hamner Institutes for Health Sciences, Research Triangle Park, NC, USA

<sup>f</sup>ScitoVation, 6 Davis Drive, PO Box 110566, Research Triangle Park, NC, USA

### Abstract

Chemical ionization plays an important role in many aspects of pharmacokinetic (PK) processes such as protein binding, tissue partitioning, and apparent volume of distribution at steady state ( $V_{d_{ss}}$ ). Here, estimates of ionization equilibrium constants (i.e.,  $pK_a$ ) were analyzed for 8,132 pharmaceuticals and 24,281 other compounds to which humans might be exposed in the environment. Results revealed broad differences in the ionization of pharmaceutical chemicals and chemicals with either near-field (in the home) or far-field sources. The utility of these high-throughput ionization predictions was evaluated via a case-study of predicted PK  $V_{d_{ss}}$  for 22 compounds monitored in the blood and serum of the U.S. population by the U.S. Centers for Disease Control and Prevention National Health and Nutrition Examination Survey (NHANES). The chemical distribution ratio between water and tissue was estimated using predicted ionization states characterized by  $pK_a$ . Probability distributions corresponding to ionizable atom types (IATs) were then used to analyze the sensitivity of predicted  $V_{d_{ss}}$  on predicted  $pK_a$  using Monte Carlo methods. 8 of the 22 compounds were predicted to be ionizable. For 5 of the 8 the predictions based upon ionization are significantly different from what would be predicted for a neutral compound. For all but one (foramsulfuron), the probability distribution of predicted  $V_{d_{ss}}$

\* strope.cory@epa.gov.

#### Disclaimer

The U.S. Environmental Protection Agency (U.S. EPA) through its Office of Research and Development funded and conducted the research described here. It has been reviewed by the U.S. EPA and approved for publication. The views expressed in this publication are those of the authors and do not necessarily represent the views or policies of the Agency. Mention of trade names or commercial products does not constitute endorsement or recommendation for use.

generated by IAT sensitivity analysis spans both the neutral prediction and the prediction using ionization. As new data sets of chemical-specific information on metabolism and excretion for hundreds of chemicals are being made available (e.g., Wetmore et al., 2015), high-throughput methods for calculating  $V_{d_{ss}}$  and tissue-specific PK distribution coefficients will allow the rapid construction of PK models to provide context for both biomonitoring data and high-throughput toxicity screening studies such as Tox21 and ToxCast.

## Keywords

pKa; high throughput; ionization; volume of distribution; PBPK

---

## 1. Introduction

Regulatory agencies worldwide are tasked with characterizing the safety of tens of thousands of commercial chemicals, yet only a small subset have been fully characterized with respect to hazard and exposure (Egeghy et al., 2012; Judson et al., 2009; USGAO, 2009; USGAO, 2013). As thousands of new chemicals are introduced into commerce each year (Judson et al., 2009; USGAO, 2009; USGAO, 2013; Wilson and Schwarzman, 2009), it becomes much more challenging to set research priorities for determining what risk, if any, these chemicals in our environment pose to human and ecological populations (Thomas et al., 2013).

High throughput, *in vitro* testing programs such as Tox21 (Tice et al., 2013) and ToxCast (Kavlock et al., 2012) have been screening thousands of chemicals for potential bioactivity. However, interpretation of these data relies on nominal tested concentration unless the results can be extrapolated to *in vivo* conditions (e.g., Wetmore et al., 2015). The Centers for Disease Control and Prevention (CDC) National Health and Nutrition Examination Survey (NHANES) includes measurements of hundreds of xenobiotic chemical concentrations in blood and serum in the U.S. population (CDC, 2012). But, without knowing how these chemicals distribute within the body, blood concentrations cannot be related to potential concentrations in tissues that might be targets of toxic effects. Further, without knowing tissue distribution, neither the total body burden of the chemical nor the rate of exposure can be estimated.

Tissue distribution of chemicals remains an important aspect of pharmacokinetics (PK) that is not rapidly measured using *in vitro* or *in vivo* techniques. Tissue PK methodologies exist in the PK literature for the prediction of chemical distribution into specific tissues or the whole body (e.g., volume of distribution at steady-state or  $V_{d_{ss}}$ ) but require specific information on physico-chemical behavior. *In silico* prediction of such chemical tissue distribution is heavily influenced by three key parameters: binding to tissue and plasma, hydrophobicity, and ionization (Peyret et al., 2010; Schmitt). Hydrophobicity (quantified by the octanol-water partition coefficient, logP) drives distribution of neutral compounds; however, a neutral compound at one pH can become ionized, for example, at a physiological pH. Thus, chemical ionization is key in estimating distribution (illustrated in Fig. 1). For predicting tissue distribution, tissues can be broadly described as consisting of components

with differing affinities for chemicals depending on the charged state of the organic chemical molecule, as shown in Fig. 1 (Peyret et al., 2010; Schmitt). The resulting ratio between the total concentration (ionized and un-ionized) of chemical in the tissue and the plasma is the distribution coefficient (logD) (Manners et al., 1988). In PK, logD is described through tissue-specific partition coefficients (PC) (Peyret et al., 2010; Schmitt).

At a given pH, some atoms of a compound can donate (dissociation) to or receive (association) protons from one or more atoms or sites within the compound (Fig. 2). Chemical association/dissociation changes the overall molecular charge, with the potential for coexistence of multiple microspecies (i.e., different charge states of the same parent molecule). The chemical association/dissociation equilibrium constant ( $pK_a$ ) characterizes the pH at which concentrations of protonated or deprotonated chemical microspecies associated with an ionizable atom or site are in equilibrium. The aim of the present work was to generate ionization profiles of chemicals at an atomic level using a rapid approach suitable for thousands of chemicals.

$pK_a$  is often reported in scientific literature as a single numerical value, sometimes categorized as “acid” or “base”. This is sufficient for a compound that undergoes a single ionization, but in many cases there are multiple ionizations, and each  $pK_a$  needs to be characterized in the range of  $0 < \text{pH} < 14$ , as shown in Fig. 2. This information is vital for PK because the overall charge and the fraction extant at a certain pH follows the Henderson-Hasselbalch equation (Hasselbalch, 1916; Henderson, 1908), which has a different behavior for acidic (negative to neutral) and basic (neutral to positive) events as pH is increased. Therefore, ionization cannot be characterized by a scalar  $pK_a$  value only, nor is it possible to compare predictions of quantitative structure–activity relationship models without further characterizing the ionization kinetics.

Understanding chemical-specific ionization properties is critical for predicting tissue distribution. As new data sets of chemical-specific information on metabolism and excretion for hundreds of chemicals are being made available (e.g., Wetmore et al., 2015), high-throughput methods for calculating  $V_{d,ss}$  and tissue-specific PK distribution coefficients will allow the rapid construction of compartmental and physiologically-based PK models. PK distribution describes how chemicals can accumulate preferentially in certain tissues, producing higher concentrations in that tissue, as characterized by tissue-specific PC. Much PK literature has been devoted to prediction of tissue PCs (Haddad et al., 2000; Peyret et al., 2010; Poulin and Krishnan, 1996a; Poulin and Krishnan, 1996b; Poulin and Theil, 2000; Rodgers et al., 2005; Rodgers and Rowland, 2006; Schmitt, 2008). These models provide the context for use and interpretation of both biomonitoring data (e.g., NHANES) and high-throughput toxicity screening studies (e.g., Tox21 and ToxCast). When appropriate PC and metabolism/physiological information are used, dynamic simulation of physiologically based pharmacokinetic (PBPK) models allows prediction of chemical concentrations in specific tissues at different times (Caldwell et al., 2012; Mumtaz et al., 2012; Pearce et al., 2017; Yoon et al., 2012)..

In this study, estimates of  $pK_a$  were generated for 32413 compounds to which humans might be exposed. This included 8132 pharmaceuticals and 24281 pesticidal, industrial and

consumer use compounds. A high-throughput method for assessing the effects of ionization on compound PK, the ionizable atom type (IAT), was used. IATs are specific configurations of atoms within a chemical that has the propensity to protonate or deprotonate. Using IATs, a probability distribution of  $pK_a$  values and therefore the probability of an atom to become ionized were estimated for 13 IATs based on predictions for all 32413 chemicals. Broad differences were identified in the ionization of chemicals intended for pharmaceutical use and chemicals with both near-field (in the home) and far-field sources. The utility of these high-throughput ionization predictions was evaluated by assessing the impact of chemical ionization on predicted  $Vd_{ss}$  for 22 NHANES chemicals using Monte Carlo sampling to explore the impact of uncertainty in the predictions for each IAT in each compound.

## 2. Materials and methods

This study uses existing ionization prediction tools (ChemAxon, SPARC, and ADMET Predictor) for a library of 32413 chemicals. The predictions are organized by IAT to characterize probability distributions for certain types of ionization events in order to perform sensitivity analysis of the predicted  $Vd_{ss}$ .

For clarification in this manuscript, the word “distribution” is used in three ways: 1) with respect to PK, the concentration of chemical in different tissues of the body (e.g., a lipophilic compound accumulating in adipose tissue); 2) in a related, but more chemistry-focused sense, it is “the overall ratio of organic and aqueous phases of a compound, ionized and un-ionized at equilibrium” (Kwon, 2001); and 3) as statistical probability distribution, i.e., a mathematical function describing the relative likelihood of a given value. To disambiguate throughout this paper, the three distributions are designated as “PK” or “tissue”, “chemical”, and “probability” distributions, respectively.

### 2.1 Chemical Library

The U.S. Environmental Protection Agency (U.S. EPA) has identified more than 50,000 chemicals, including many synthetic chemicals, to which humans might be significantly exposed (Richard and Williams, 2002). These chemicals cover a variety of use classes such as consumer products, food additives, and human and veterinary drugs and were collected from the following sources, with significant overlap:

- 43,596 chemicals with documented use, and therefore exposure potential, stored in the Chemical and Product Categories (CPCat) database (Dionisio et al., 2015), which is part of the Aggregate Computational Toxicology Repository (ACToR) system (Judson et al., 2008; Judson et al., 2012).
- A list of approximately 15,000 curated chemical structures for multiple inventories of environmental interest in the DSSTox collection of structures from the public DSSTox (Richard and Williams, 2002). In particular, structures for all of the ToxCast (Dix et al., 2007) and Tox21 (Collins et al., 2008) chemicals were included.
- The Canadian domestic substances list (DSL) (Environment and Climate Change Canada, 2016) and a list of all substances (~ 24,000 chemicals) thought to be in

commerce in Canada, including chemicals with potential for human or ecological exposure (Health Canada, 2009).

- Approximately 10,000 chemicals from the Endocrine Disruptor Screening Program (EDSP) Universe of Chemicals. U.S. EPA's EDSP is required to test certain chemicals for endocrine-disrupting potential, in particular, through the estrogen receptor (Fenner-Crisp et al., 2000).
- A list of approximately 15,000 chemicals from PHYSPROP data sets with valid structures and after removal of duplicates (Mansouri et al., 2016; USEPA, 2015).

A KNIME structure-standardization workflow was used to process these lists of chemicals (Mansouri et al., 2016). To characterize any potential differences in the lists, the ACToR Use Categories (Dionisio et al., 2015) were used to assign chemicals to pharmaceutical, near- and far-field environmental chemical classes. The ACToR Use Categories were developed using data from federal, state, and international regulatory listings of chemicals in specific classes. Chemicals were assigned to specific use categories by tabulating the number of times a chemical fell into a category in all of the regulatory listings. A chemical was assigned to a category if it fell into that category three or more times. If it passed the “three-hit” threshold for more than one category, the chemical was assigned to multiple categories.

In this study, pharmaceutical compounds were considered pharmacologically active substances intended for internal or external use for the treatment and prevention of disease. Whether the pharmaceuticals failed or succeeded to be introduced commercially was not a consideration. Environmental compounds were separated into those with near- and far-field sources (e.g., in the home vs. industrial release) (Arnot et al., 2006). Table 1 gives a general overview of the classification scheme for each chemical type.

## 2.2 pK<sub>a</sub> predictions

The Marvin pK<sub>a</sub> plug-in from ChemAxon (Cambridge, MA, USA) was selected for predicting pK<sub>a</sub> in this research (Szegezdi and Csizmadia, 2007; Szegezdi and Czismadia, 2004). ChemAxon's Marvin pK<sub>a</sub> plug-in uses only three atomic descriptors (partial charge, atomic polarizability, and structure-specific increments) with nonlinear relationships to predict the pK<sub>a</sub> microconstants, which are subsequently used to obtain the macroconstants (Szegezdi and Csizmadia, 2007; Szegezdi and Czismadia, 2004). The plug-in also reports the position in the chemical simplified molecular-input line-entry system (SMILES) string (or visualization interface showing the molecule itself), specifying the atom that becomes ionized for each pK<sub>a</sub>. Functional groups identified with ADMET Predictor (Simulations Plus, Buffalo, NY, USA) were used to organize types of ionizations, allowing sensitivity analysis (Simulations Plus, 2017).

In addition to predictions made using the ChemAxon pK<sub>a</sub> plug-in, pK<sub>a</sub> predictions from SPARC Performs Automated Reasoning in Chemistry (SPARC; ARChem, Danielsville, GA, USA) and ADMET Predictor were also compared (Supplemental Figure S1). For compounds that both accept and donate protons due to microconstant transitions between chemical microspecies, SPARC and ADMET Predictor report the ionization as a “mixed” pK<sub>a</sub>. This “mixed” category adds ambiguity to the predictions because it requires an

inference mechanism to relabel the mixed  $pK_a$  predictions and thus makes the calculation of the Henderson-Hasselbalch equation unclear. Hence, only the ChemAxon Marvin  $pK_a$  plug-in results were used in our analysis. See the appendix for a discussion of  $pK_a$  prediction paradigms.

### 2.3 Ionizable Atom Types

A two-dimensional representation of a chemical was generated using SMILES (Helson, 2007; Weininger, 1988) to identify the specific atoms associated with the  $pK_a$  value and the atoms' protonation/deprotonation action. ADMET Predictor identified 82 functional groups, each one containing a fingerprint of the atomic configurations for which a specific atom will become ionized. These configurations are referred to as putative IATs. Note that IATs are atom-centric, where only the ionizable atom of a chemical and that atom's local neighborhood were considered, not the molecule as a whole. This allowed clear labeling of each  $pK_a$  as proton donating (acidic  $pK_a$ ;  $apK_a$ ) or accepting (basic  $pK_a$ ;  $bpK_a$ ). The ionizable atom and its atomic neighborhood formed a fingerprint of a specific type of ionization event, which will be referred to as the IAT signature.

A library of SMILES substrings was developed using the SMILES strings for compounds with an IAT predicted using ADMET Predictor (Simulations Plus, 2017). These SMILES substrings were then used to create a library of signatures for 13 commonly predicted IATs. These signatures identify putative ionizable sites in SMILES strings of unknown chemicals and further specify the maximal putative IAT the SMILES signature represented, *e.g.*, the IAT routine will not identify a hydroxyl group (-OH) that is part of the larger carboxyl group (-COOH). The putative IATs are confirmed to be a true IAT if and only if the atom has a covalent bond available to accept or donate a hydrogen atom. If so, then the atom is added to its corresponding IAT library.

After building IAT libraries, two parameters were derived: (i) the frequency that an IAT is ionized in the [0, 14] pH range and (ii) the probability distribution of predicted  $pK_a$  values associated with the IAT. IATs were assumed, by inspecting the resulting distributions, to be normally distributed.

### 2.4 Prediction of Tissue Distribution

PCs of chemical-specific tissue to free fraction in plasma ( $PC_{T,p}$ ) were predicted using the method of Peyret et al. (2010). Tissue specificity was based on the cellular fraction of total volume; the water, lipid, and protein fraction of cellular volume; and the fractions of types of lipid (Peyret et al., 2010). Chemical specificity was based on (i) the octanol-water PC ( $P_{ow} = e^{\log P}$ ) obtained from the ChemAxon  $pK_a$  Plug-in and (ii) ionization scheme: neutral chemical model, the IAT- and ChemAxon  $pK_a$  Plugin-based association/dissociation constants.

The tissue:plasma PCs ( $PC_{T,p}$ ) were determined from

$$PC_{T:p} = \frac{F_{ct}PC_{ctw} + F_{it}PC_{itw}}{F_pPC_{pw} + F_ePC_e}, \quad (1)$$

where the subscripts denote the matrices ( $m$ ) cellular tissue ( $ct$ ), interstitial fluid ( $it$ ), erythrocytes ( $e$ ) and plasma ( $p$ );  $F_m$  is the percent of the tissue comprised by each matrix;  $PC_{mw}$  is the PC for each matrix (Peyret et al., 2010), and  $T$  is the set of tissues parameterized in Schmitt (2008).

The PC for each matrix  $m$  was predicted as (Peyret et al., 2010):

$$PC_{mw} = \frac{(1 + I_m) \cdot F_{wm} + P_{ow} \cdot F_{nlm} + I_m \cdot PC_{aplw} \cdot F_{apl} + (1 + I_m) \cdot PC_{prw} \cdot F_{prm}}{(1 + I_w)}, \quad (2)$$

where each matrix  $m$  is comprised of the following constituents ( $c$ ): water ( $w$ ), neutral lipids ( $nl$ ), acidic phospholipids ( $apl$ ), and protein ( $pr$ );  $F_{cm}$  is the fraction of each matrix  $m$  comprised of each constituent  $c$ ;  $P_{ow}$  is the octanol:water partition coefficient;  $PC_{aplw}$  is set to zero for interstitial fluids and plasma where it is assumed no acidic phospholipids exist, and otherwise is predicted as the blood:plasma ratio scaled by the erythrocyte content, since erythrocytes provide binding pockets that are similar to acidic phospholipids to bind basic compounds; and  $PC_{prw}$  is binding by albumin and lipoproteins as characterized by unbound fraction in plasma ( $F_u$ ).  $w$  is water,  $m$  is the matrix,  $nl$  is neutral lipids,  $apl$  is acidic phospholipids, and  $pr$  is protein (Peyret et al., 2010). Each variable in Eq. (2) also had an indicator function (not shown) to ensure that biologically implausible partitioning did not occur. In Figure 1, the presence of an arrow from C, N, and A to a matrix represents the indicator function equal to 1, lack of an arrow represents the indicator function set to 0.  $I_m$  is the variable influenced by  $pK_a$  and represents the ratio of the concentration of the chemical in the ionized state to the concentration in the neutral form for a given  $pK_a$ -pH pair. The Henderson-Hasselbalch equation is utilized to calculate the  $I_m$ , where

$$I_m = \begin{cases} 0 & \text{neutral} \\ 10^{\text{pH}-\text{pKa}} & \text{monoprotic acids} \\ 10^{\text{pKa}-\text{pH}} & \text{monoprotic bases} \\ 10^{2\text{pH}-\text{pKa}_2-\text{pKa}_1} + 10^{\text{pH}-\text{pKa}_1} & \text{diprotic acids} \\ 10^{\text{pKa}_1+\text{pKa}_2-2\text{pH}} + 10^{\text{pKa}_1-\text{pH}} & \text{diprotic bases} \\ 10^{\text{pH}-\text{apKa}} + 10^{\text{bpKa}-\text{pH}} & \text{zwitterions} \\ \vdots & \vdots \end{cases}, \quad (3)$$

and pH varies according to tissue as in Schmitt (2008). Note that Eq. (2) is an extension of the calculation of logD, which is equal to logP for neutral compounds, but incorporates ionization through taking the log of the sum of the concentrations of ionized and non-

ionized compounds in octanol divided by the sum of the concentrations of ionized and non-ionized compounds in water.

A special case of equations were used for highly lipophilic organic compounds (HLOC). In these cases, the logP and tissue lipid content dominated the partition coefficient calculations. Equations can be found in (Haddad et al., 2000; Poulin and Haddad, 2012).

With the partition coefficients in hand, the  $V_{d_{ss}}$  can be calculated. The  $V_{d_{ss}}$  (in L/kg bodyweight) for serum or blood reflects the aggregate tissue distribution of a chemical for the whole body. The calculation of the  $V_{d_{ss}}$  is the predicted PCs scaled by physiological tissue volumes:

$$V_{d_{ss}} = V_{plasma} + \sum_{T \in Tissue} V_T PC_{T:p} \quad (4)$$

where  $V_T$  is the percentage volume of a tissue (in kg, obtained from Schmitt (2008)), and  $PC_{T:p}$  is the PC for the tissue.

## 2.5 Sensitivity Analysis Using IAT Probability Distributions

The utility of high-throughput ionization predictions is evaluated by examining the importance of correctly determining the effect of chemical ionization on predicted  $V_{d_{ss}}$  for environmentally relevant chemicals. IAT probability distributions, the assumption of chemical neutrality, and the point estimates obtained by ChemAxon  $pK_a$  Plugin are compared in a sensitivity analysis of ionization effects using the  $V_{d_{ss}}$  derived from the predicted PCs as the reporter parameter.

A Monte Carlo sampling with replacement strategy (bootstrapping), implemented in R (version 3.3.2), used the developed  $pK_a$  probability distributions associated with IATs, to perform a sensitivity analysis of the effects of  $pK_a$  values on the apparent  $V_{d_{ss}}$  using the tissue-based PC calculations of Peyret et al. (2010). Although many modern tools for predicting  $pK_a$  attempt to characterize the uncertainty in their predictions, these characterizations are by necessity based on performance using the available training set, and most training sets are focused on pharmaceutical chemicals (Liao and Nicklaus, 2009). For this reason, an alternative approach was used in this study that focused on the probability distribution for chemicals predicted to have specific IATs.

The sensitivity analysis was performed on a set of chemicals from the NHANES (CDC, 2012), which include 109 compounds in the blood and serum of the U.S. population tracked by NHANES. Of the 109 chemicals, 22 have the necessary parameters needed for PC calculation, particularly  $F_u$  in plasma, shown in Table 2 (Wetmore et al., 2015; Wetmore et al., 2012)].

## 3. Results

$pK_a$  predictions were generated for the 32413 chemicals. Fig. 3 illustrates the number of association and dissociation actions of these chemicals using the predicted  $pK_a$  values derived from ChemAxon versus the pH at which the ionization occurs. This also shows the



acidic/basic  $pK_a$  predictions as a function of chemical class. The ionization profiles of pharmaceutical compounds versus compounds with potential near- and far-field environmental sources were distinct: Far-field chemicals had the broadest range of  $pK_a$  values, while pharmaceuticals had the narrowest (Table S1). Pharmaceutical compounds have a distinct  $bpK_a$  (potential to become positively charged) mode with the peak just above the physiologically relevant pH at or near 7.4, whereas the far-field chemicals have modes that peak on either side of pH 7.4. This difference is interesting in the context of PCs because the mode of the  $bpK_a$  ionization for pharmaceutical compounds is very close to the plasma pH of the tissue-based PC prediction method used in this analysis (Peyret et al., 2010); this peak indicates that partitioning into acidic phospholipids could play a large role in pharmaceutical compound tissue distribution.

Of the three classes, pharmaceutical compounds have the highest propensity to be ionized (87% [6,751 of 7,766] of all pharmaceuticals are ionizable; Table S1). The near-field environmental chemicals have the fewest compounds that are ionized, with well over half of the chemicals being non-ionizable (Table S1). Note also that of the predicted ionizable sites, the  $pK_a$  values show relatively few ionized sites at the physiological pH, i.e., a strong dip between the modes at  $6 < \text{pH} < 8$ .

Chemicals that were predicted to be charged, with  $pK_a$  outside the 0–14 pH range (i.e., very strong/weak acids or bases), are designated as “terminally ionized.” As shown in Fig. 3, the probability distribution of non-terminally ionized  $pK_a$  values that are predicted in far-field chemicals closely resembles the pharmaceutical compound probability distribution, with modes around 4, 10, and 14. Far-field environmental chemicals, however, have a stronger tendency toward low  $pK_a$  values compared to the pharmaceuticals, likely due to, *e.g.*, sulfur compounds such as surfactants.

Chemicals predicted to be terminally ionized, particularly those with  $pK_a$  much less than zero, were predominantly far-field environmental chemicals. Further investigation is needed to determine whether the  $pK_a$  values for these compounds were truly extreme values, or whether the structures of the compounds were so different from the training sets used in the models that they produced erroneous values (i.e., outside the models’ domain of applicability).

### 3.1 IAT identification and parameterization

Fig. 4 shows the average number of occurrences for a subset of IATs for all chemicals, normalized by the total number of chemicals in each class. These are then sorted from low to high by the average number of IATs identified per chemical in the pharmaceutical class. These values are the expected number of each IAT per compound in each chemical class. Chemical classes tend to have differing IAT compositions and IAT loads (Fig. S2). This is true particularly for highly represented groups such as aliphatic hydroxyls, ethers, amides, and aromatic nitrogens. Pharmaceuticals also tend to be enriched in aliphatic IATs (aliphatic hydroxyl, aliphatic primary amines, and aliphatic carboxyl), potentially reflecting the propensity for anabolic pathways in these compounds. Far-field compounds tend to be enriched in aromatic IATs found in several environmental compounds (aromatic hydroxyl, aromatic primary amines, and aromatic carboxyl), possibly reflecting the properties of the

compounds in which they occur. Lipophilicity, for example, is desirable for solvents, but is less desirable in pharmaceuticals. Other IATs of note in environmental compounds are sulfonates, ethers, and NO<sub>2</sub> nitrogens commonly found in surfactants. Near-field environmental chemicals tend to have the lowest concentration of IATs, although these chemicals are enriched in sulfur-containing IATs.

Fig. 5 shows the density of predictions from the ChemAxon p*K<sub>a</sub>* Plugin for the selected IATs in Fig. 4. Table 3 shows the fraction of times each IAT pattern is ionized versus the total number identified in the SMILES string. This illustrates the number of each IAT predicted to be ionized versus the total IAT predicted by the ChemAxon p*K<sub>a</sub>* Plugin and the resulting percentage of the IAT that is associated with an ionization. The probability distribution of IAT p*K<sub>a</sub>* values in Figure 5 captures the variability in p*K<sub>a</sub>* prediction given the surrounding neighborhood of the IAT.

In general, the IAT functional groups with well-defined probability distributions have a high percentage of p*K<sub>a</sub>* values predicted for the IAT. Examples include, the carboxyls (97.3%; AICbxyl-COOH), aromatic hydroxyls (72.5%; ArHdxl-OH), tertiary amines (81.6%; TerAmine->N-), and primary aliphatic amines (91.7%; PriAmAli\_-NH2). Other IATs, however, are rarely protonated/deprotonated, such as aliphatic hydroxyls (42.8%; AlHdxl-OH), primary aromatic amines (53.7%; PriAmAro\_-NH2), and especially ethers (10.1%; Ether\_-O-). It is interesting to note that the percentage ionized tends to correspond with how close the IAT probability distribution tends to the middle of the p*K<sub>a</sub>* range.

Several of the IATs in Fig. 5 show tight probability distributions for predicted p*K<sub>a</sub>* values, and this suggests that there is little variability in their atomic neighborhoods. Chief among these tight distributions are the aliphatic carboxyls (AICbxyl-COOH) and primary aliphatic amines (PriAmAli\_-NH2), both of which are terminal atom groups with lognormal distributed predictions. Ethers (Ether\_-O-) and aliphatic hydroxyls (AlHdxl-OH) also share this behavior, but most of these IATs do not become ionized (10.1% and 42.8%, respectively) compared to the terminal groups above (97.3% and 91.7%, respectively), possibly because all instances of the relatively noncomplex atomic fingerprints were captured. The aromatic hydroxyl (ArHdxl-OH) probability distribution also displayed a well-defined peak, yet with greater variance than other compounds, likely due to the variable aromatic ring structure neighborhoods in which they occur.

Most IAT probability distributions in Fig. 5 show subtle differences between the chemical classes. Pharmaceutical compound IATs tend to prevent the compounds from distributing into some tissues, such as fat, that would result in longer half-lives. Pharmaceuticals have: (1) a higher proportion of negatively charged IATs, such as the carbonyls (Carbonyl\_C=O) and aliphatic carboxyls (AICbxyl-COOH); and (2) a lower proportion of positively charged aliphatic IATs (i.e., primary aliphatic amines (PriAmAli\_-NH2), secondary amines (SecAmine->NH), and tertiary amines (TerAmine->N-); do not get partitioned in to acidic phospholipids). Note also that pharmaceuticals have a higher proportion of positively charged primary aromatic amines. This is likely due to the fact that there are relatively few primary aromatic amine (PrimAmAro\_-NH2) IATs, and small sample size causes the average number of these positively charged IATs in pharmaceutical compounds to appear

higher (as shown in Fig. 3, Fig. S2). Additionally, as seen in the primary Amine (PriAmine\_  
NH<sub>2</sub>) panel, less than half of these are charged ( $pK_a < \sim 5$ ) rather than uncharged ( $pK_a > \sim 9$ ). Finally, several IATs have wide probability distributions. In particular, aromatic nitrogens (ArNitrog\_  
=N-) follow no apparent parametric distribution, and secondary amines (SecAmine\_  
>NH) have one mode around pH 10 but also have uniformly distributed predictions along the remainder of the pH spectrum suggesting that these IATs are more complex than the simple local neighborhood approach taken in this analysis.

### 3.2 Sensitivity Analysis of Ionization and Volume of Distribution

Fig. 6 shows the results of the Monte Carlo analysis to assess how the uncertainty in the  $pK_a$  value affects the  $V_{d_{ss}}$  for the NHANES chemicals for which we have sufficient information to make predictions (namely, fraction unbound in plasma,  $F_u$ ). Fig. 6 compares the apparent  $V_{d_{ss}}$  for probability distributions of the chemicals in Fig 5 that result from sampling  $pK_a$  values with replacement from the IAT probability distribution associated with a given IAT on a molecule.

The red dots in Fig. 6 indicate the  $V_{d_{ss}}$  for that chemical based on its exact ChemAxon predictions, while the box-and-whisker plots (with black dots indicating outliers beyond 1.5 \* interquartile range (Tukey, 1977)) indicate the range of  $V_{d_{ss}}$  from the sensitivity analysis. The blue dots in Fig. 6 indicate the  $V_{d_{ss}}$  if ionization had been ignored altogether. For example, the median, canonical, and neutral  $V_{d_{ss}}$  values of BPA tend to cluster around approximately 80 L/kg.

The neutral chemical assumptions and the predictions from ChemAxon are often overlapping (Fig. 6) and this is clearly seen for neutral chemicals. However, for five of the eight ionizable compounds, the neutral assumptions and the ChemAxon predictions are significantly different (e.g., atrazine). For all but one of the chemicals in Fig. 6, the probability distribution of predicted  $V_{d_{ss}}$  generated by IAT sensitivity analysis spans both the neutral prediction and the prediction based on the ChemAxon prediction. When there is a significant difference (e.g., foramsulfuron), our  $pK_a$  sensitivity analysis method overestimates  $V_{d_{ss}}$ , which might be health-protective since low volumes of distribution increase the probability of metabolic clearance (Smith et al., 2015).

The predicted  $V_{d_{ss}}$  of BPA in this analysis is overpredicted when compared to literature estimates which range from 4.6 to approximately 27.0 L/kg, depending on the route that the dose was administered (Kurebayashi et al., 2003; Yoo et al., 2000). This overprediction is more likely due to the PC estimation than to ionization. The prediction of PCs assumes that tissue distribution is by diffusion only and does not consider transporters, which can alter the partitioning of BPA and its primary metabolite BPA glucuronide (Mazur et al., 2012; Moscovitz et al., 2016; Teegarden et al., 2005), potentially lowering its  $V_{d_{ss}}$ .

For the non-ionizing chemicals in Fig. 6, denoted by (N), the red dot and box-and-whisker plots overlap. Some neutral chemicals such asalachlor, acetochlor, and metalochlor have outlying points that are likely due to mispredicted carbonyl (Carbonyl\_C=O) groups. These groups can make the chemical acidic, which can in turn prevent partitioning into adipose

tissue. The median value is unaffected since only 6.7% of the carbonyls are predicted to be ionized despite the predicted carbonyl groups.

Among the ionized compounds, the range for  $V_{d_{ss}}$  was wider or narrower depending on compound. In Fig. 6, compounds varied due to the interplay between various ionizable sites, i.e., chemicals with multiple  $pK_a$ s, in general, have wide distributions. Most notably, Bisphenol A has identical sites that can become charged. The neutral chemicals that have wide ranges have IATs with a low likelihood of ionization. For example, Ethers and Carbonyls become negatively charged, which essentially removes the lipid compartment from the equation.

## 4. Discussion

A major challenge in assessing any risk posed by thousands of untested and unmeasured chemicals is cost-efficient predictive models (National Academies of Sciences and Medicine, 2017). PK methods are needed to keep pace with expanded biomonitoring data (i.e., exposure) and high-throughput screening (i.e., hazard). High-throughput methods allow for prediction of key PK properties such as  $V_{d_{ss}}$  and tissue-specific PK distribution coefficients (Haddad et al., 2000; Peyret et al., 2010; Poulin and Krishnan, 1996a; Poulin and Krishnan, 1996b; Rodgers et al., 2005; Rodgers and Rowland, 2006; Schmitt, 2008). However, these models require measurement or prediction of chemical ionization, as characterized by  $pK_a$ . Here we have examined the predicted ionization properties for 32413 compounds. These data revealed broad differences between pharmaceuticals and those chemicals with either near-field (in the home) or far-field sources. The introduction of distributions for specific ionizable atom types (IATs) allowed sensitivity analysis via Monte Carlo sampling. As an example, we evaluated the sensitivity of predicted  $V_{d_{ss}}$  to chemical ionization predictions on  $V_{d_{ss}}$  for NHANES compounds.

The  $V_{d_{ss}}$  values in Table 2 allow inference of body burden from measured concentrations in blood or serum. Further, if rates of metabolism and excretion can be determined, as done by Wetmore et al. (2015), then sufficient information is available for parameterizing a “one compartment” PK model. If the PCs are handled separately rather than as an aggregate  $V_{d_{ss}}$ , a PBPK model can be constructed. This high-throughput method for calculating  $V_{d_{ss}}$  and tissue-specific distribution coefficients allows the rapid construction of PK models to provide context for both biomonitoring data and toxicity screening study data such as Tox21 and ToxCast.

In the current study we assumed that text mining using regular expression libraries captured all patterns that determine IAT in SMILES strings. We further assumed that the application of ADMET Predictor IAT predictions is consistent with the algorithmically different ChemAxon  $pK_a$  plug-in. Neither of these assumptions, however, affected a significant portion of the compounds in our chemical list ( $\cong 0.8\%$ ). Nevertheless, it should be noted that for high-throughput and data-poor analyses, such assumptions are inevitable in order to make useful inferences. If an assumption is wrong, the prediction are likely to be inaccurate.

Another assumption is that the CAS Registry numbers (CASRN) are correct and associated with the appropriate chemical structures. In fact, CASRN might be associated with incorrect chemical SMILES strings; often, a single chemical can have several CASRN, or one CASRN is associated with several different chemicals. This work resolves this issue by developing and applying a set of rules to make unique CASRN-to-chemical assignments, which has the potential to make erroneous assignments of ACToR UseDB category terms to chemicals. This, in turn, affected the chemical class portion of this analysis. However, such changes potentially occurred to fewer than 300 chemicals, or approximately 1% of the data set, and therefore are unlikely to change the analysis significantly.

Previous analyses of  $pK_a$  method sensitivity (Liao and Nicklaus, 2009) that are based on small subsets of only pharmaceutical compounds. Here we have used our large library of primarily environmental compound predictions to develop probability distributions for specific IATs. These IAT distributions allow for sensitivity analysis via Monte Carlo simulation to quantify the potential uncertainty that can be attributed to each predicted  $pK_a$ . Wide distributions for predicted values (e.g.,  $Vd_{ss}$ ) are indicative of greater uncertainty, compared to chemicals with tight distributions. Such considerations can inform in chemical prioritization.

A strength of the IAT method is that the data is not restricted to a specific set of chemicals. Though we chose to use a large dataset of environmental compounds, any large dataset of chemicals could be substituted to derive the IAT distributions. Hence, this method could be extended to pharmaceutical  $pK_a$  predictions or derived from regulatory datasets).

Sensitivity analysis by sampling substitute  $pK_a$  values from an IAT probability distribution has potential positive and negative consequences. One positive outcome is that a large range of most likely volumes of distribution will be represented by our predictions, which is demonstrated by: (1) the span of predictions containing both the neutral and the ChemAxon  $pK_a$  plug-in predictions (e.g., atrazine, BPA, oxasulfuron, carbaryl); and, (2) cases where both our method and the ChemAxon  $pK_a$  plug-in have the same prediction for the ionized form of the chemical (e.g., 2,4-dichlorophenoxyacetic acid). On the other hand, it is possible that predictions made by our method will fall outside the neutral and  $pK_a$  plug-in ionization predictions.

For example, our method overpredicts acephate vs  $pK_a$  plug-in, but the prediction is much closer than for foramsulfuron. Foramsulfuron is an extreme case: For the neutral prediction, in Equation 2,  $P_{ow}F_{nlm}$  is the only non-zero term in the numerator and, due to the low  $\log P$ , is a small value (no ionization, hence denominator = 1). For the ionized term, the  $pK_a$  Plugin value for the secondary amine group, 3.46, is several orders of magnitude lower than the peak of the secondary amine (SecAmine\_ $\rightarrow$ NH) probability distribution ( $\sim 9.5$ ; Fig. 5) peak. In this case, the term for the neutral partitioning is set to zero, and the numerator is only acidic phospholipid partitioning, scaled by the value of  $I_m = 10^{pK_a - pH} = 10^{3.46 - 7.4} = 1.1 \times 10^{-4}$ . Hence, the ionized  $Vd_{ss}$  is lower than the neutral  $Vd_{ss}$ . Our prediction has three possible secondary amine groups in the foramsulfuron molecule. For any predicted ionizations, the value chosen will likely be orders of magnitude higher than the  $pK_a$  predicted by  $pK_a$  Plugin, and hence will have much larger values of  $I_m$  in the numerator,

which explains the overpredictions. Acephate is overpredicted for the same reasons. The  $pK_a$  predicted by  $pK_a$  Plugin is 6.54, still two orders of magnitude lower than the SecAmine (SecAmine\_>NH) peak but close enough to the physiological pH of 7.4 to cause approximately 10 % of the IATs to be ionized.

A limitation in sensitivity analysis based upon sampling IAT probability distributions are the tails of the probability distributions. For example, the amide (Amide\_C(=O)N<) IAT of oxasulfuron. In this instance, the amide in oxasulfuron is in a configuration such that the  $pK_a$  for the ionizable atom is predicted at the extreme of the amide IAT probability distribution, approximately a full 10 units of the pH scale away from the mean of the probability distribution. Hence, a  $pK_a$  value > 7.5 sampled from the amide IAT probability distribution, which causes the amide to be negatively charged at the physiological range, will negate any partitioning into acidic phospholipids and thus lower the  $V_{d_{ss}}$ . As was shown, the probability distribution of mis-predictions still showed signatures of certain IAT configurations, particularly with compounds that should be neutral (e.g., phthalates). In such cases, computational post-hoc classification could be used to modify the predicted  $V_{d_{ss}}$  based on a set of rules for a given IAT configuration.

Sensitivity analyses also rest upon the ability to parameterize the models used the analyses. The method presented here relies on pharmacokinetic parameters. Most such parameters can be either predicted in silico (e.g., logP) or found in literature. However, current in silico predictors for parameters such as  $F_u$  either have been developed exclusively using pharmaceutical chemicals or currently rely on proprietary descriptors that are not available for all chemicals of interest (Ingle et al., 2016).

Further improvements to the IAT distributions themselves could be obtained by using more of the chemical neighborhood and 3D structures of the chemicals to get finer granularity (e.g., Geidl et al. (2015), Bochevarov et al. (2016)). This could potentially make tighter IAT  $pK_a$  probability distributions by, e.g., splitting  $pK_a$  probability distributions such as the aromatic nitrogens (ArNitrogen\_=N-) and secondary amines (SecAmine\_>N) on such higher order chemistries.

Future work to parameterize simple PBPK models through prediction of PK distribution into specific tissues (i.e., tissue partitioning) can proceed by considering the relationship between logP and  $pK_a$  (expressed through the logD parameter), absorption, metabolic clearance, and the plasma binding ( $F_u$ ). The plasma binding has a large effect in tissue-composition-based PC prediction methods that rely on  $F_u$  to determine the partitioning (Schmitt (2008)). When plasma protein binding data are available or are predicted (Ingle et al., 2016), the techniques presented here for profiling  $pK_a$ , allow high-throughput, computationally inexpensive prediction of the apparent  $V_{d_{ss}}$ .

This study has identified differences between broad classes of chemicals through consideration of predicted ionization as characterized by  $pK_a$ . These ionization predictions have been understood in terms of the occurrence of specific IATs. By characterizing the probability distribution of predictions for key IATs across an extensive chemical library, we are now able to perform sensitivity analysis for chemical properties that depend upon  $pK_a$

predictions. As an example, we have predicted  $V_{d_{ss}}$  for chemicals monitored in the blood and serum of the U.S. population by NHANES. These predictions inform the chemical body burden indicated by biomonitoring data. Importantly, sensitivity analysis based upon IAT probability distributions informs confidence in a manner that is suitable for application to thousands of chemicals that may be in the environment.

## Supplementary Material

Refer to Web version on PubMed Central for supplementary material.

## Acknowledgments

The Oak Ridge Institute for Science and Education provided funding for K. Mansouri and initially for C. Strope (EPA-ORD/NCCT-2012-05) before continuing at the Hamner Institutes for Health Sciences. The U.S. Environmental Protection Agency through its Office of Research and Development funded and managed a portion of the research described here, with support for J.F. Wambaugh, J.R. Rabinowitz, and C. Stevens.

We would like to thank Thomas Peyret for sharing the Excel spreadsheets with the code needed to correctly predict the PC predictions using his method. We would like to thank Eric Watt for several helpful discussions that focused our work. We appreciate feedback from Antony Williams and Brandall Ingle in preparation of this manuscript. We appreciate technical editing from Stacy Henkle as well as American Journal Experts.

## References

- Arnot JA, MacKay D, Webster E, Southwood JM. Screening level risk assessment model for chemical fate and effects in the environment. *Environmental science & technology*. 2006; 40:2316–2323. [PubMed: 16646468]
- Bochevarov AD, Harder E, Hughes TF, Greenwood JR, Braden DA, Philipp DM, et al. Jaguar: A high-performance quantum chemistry software program with strengths in life and materials sciences. *International Journal of Quantum Chemistry*. 2013; 113:2110–2142.
- Bochevarov AD, Watson MA, Greenwood JR, Philipp DM. Multiconformation, Density Functional Theory-Based p K a Prediction in Application to Large, Flexible Organic Molecules with Diverse Functional Groups. *Journal of Chemical Theory and Computation*. 2016; 12:6001–6019. [PubMed: 27951674]
- Caldwell JC, Evans MV, Krishnan K. Cutting edge PBPK models and analyses: providing the basis for future modeling efforts and bridges to emerging toxicology paradigms. *Journal of toxicology*. 2012
- CDCNational Health and Nutrition Examination Survey 2012
- Collins FS, Gray GM, Bucher JR. Transforming environmental health protection. *Science (New York, NY)*. 2008; 319:906.
- Dionisio KL, Frame AM, Goldsmith M-R, Wambaugh JF, Liddell A, Cathey T, et al. Exploring consumer exposure pathways and patterns of use for chemicals in the environment. *Toxicology Reports*. 2015; 2:228–237. [PubMed: 28962356]
- Dix DJ, Houck KA, Martin MT, Richard AM, Setzer RW, Kavlock RJ. The ToxCast program for prioritizing toxicity testing of environmental chemicals. *Toxicological Sciences*. 2007; 95:5–12. [PubMed: 16963515]
- Doucette WJ. Quantitative structure-activity relationships for predicting soil-sediment sorption coefficients for organic chemicals. *Environmental Toxicology and Chemistry*. 2003; 22:1771–1788. [PubMed: 12924577]
- Eckert F, Klamt A. Accurate prediction of basicity in aqueous solution with COSMO-RS. *Journal of computational chemistry*. 2006; 27:11–19. [PubMed: 16235262]
- Eckert F, Leito I, Kaljurand I, Kütt A, Klamt A, Diedenhofen M. Prediction of acidity in acetonitrile solution with COSMO-RS. *Journal of computational chemistry*. 2009; 30:799–810. [PubMed: 18727157]

- Egeghy PP, Judson R, Gangwal S, Mosher S, Smith D, Vail J, et al. The exposure data landscape for manufactured chemicals. *Sci Total Environ*. 2012; 414:159–66. [PubMed: 22104386]
- Elyashberg M, Blinov K, Smurnyy Y, Churanova T, Williams A. Empirical and DFT GIAO quantum-mechanical methods of <sup>13</sup>C chemical shifts prediction: competitors or collaborators? *Magnetic Resonance in Chemistry*. 2010; 48:219–229. [PubMed: 20108257]
- Environment and Climate Change Canada Domestic Substances List 2016
- Fenner-Crisp PA, Maciorowski AF, Timm GE. The endocrine disruptor screening program developed by the US Environmental Protection Agency. *Ecotoxicology*. 2000; 9:85–91.
- Fraczkiewicz R, Lobell M, Göller AH, Krenz U, Schoenneis R, Clark RD, et al. Best of Both Worlds: Combining Pharma Data and State of the Art Modeling Technology To Improve in Silico p K a Prediction. *Journal of chemical information and modeling*. 2014; 55:389–397. [PubMed: 25514239]
- Franco A, Fu W, Trapp S. Influence of soil pH on the sorption of ionizable chemicals: modeling advances. *Environmental Toxicology and Chemistry*. 2009; 28:458–464. [PubMed: 18937533]
- Franco A, Trapp S. Estimation of the soil–water partition coefficient normalized to organic carbon for ionizable organic chemicals. *Environmental Toxicology and Chemistry*. 2008; 27:1995–2004. [PubMed: 18384236]
- Geidl S, Svobodová Va eková R, Bendová V, Petrussek Ls, Ionescu C-M, Jurka Z, et al. How does the methodology of 3D structure preparation influence the quality of p K a prediction? *Journal of chemical information and modeling*. 2015; 55:1088–1097. [PubMed: 26010215]
- Haddad S, Poulin P, Krishnan K. Relative lipid content as the sole mechanistic determinant of the adipose tissue: blood partition coefficients of highly lipophilic organic chemicals. *Chemosphere*. 2000; 40:839–843. [PubMed: 10718576]
- Hasselbalch KA. Die Berechnung der Wasserstoffzahl des Blutes aus der freien und gebundenen Kohlensäure desselben, und die Sauerstoffbindung des Blutes als Funktion der Wasserstoffzahl: Julius Springer; 1916
- Health Canada Final Integrated Framework for the Health-Related Components of Categorization of the Domestic Substances List Under CEPA 1999 2009
- Helson HE. Structure diagram generation. *Reviews in Computational Chemistry*. 2007; 13:313–398.
- Henderson LJ. Concerning the relationship between the strength of acids and their capacity to preserve neutrality. *American Journal of Physiology--Legacy Content*. 1908; 21:173–179.
- Ingle BL, Veber BC, Nichols JW, Tornero-Velez R. Informing the Human Plasma Protein Binding of Environmental Chemicals by Machine Learning in the Pharmaceutical Space: Applicability Domain and Limits of Predictability. *Journal of Chemical Information and Modeling*. 2016; 56:2243–2252. [PubMed: 27684444]
- Jelfs S, Ertl P, Selzer P. Estimation of p K a for druglike compounds using semiempirical and information-based descriptors. *Journal of chemical information and modeling*. 2007; 47:450–459. [PubMed: 17381168]
- Jover J, Bosque R, Sales J. QSPR prediction of pKa for benzoic acids in different solvents. *QSAR & Combinatorial Science*. 2008; 27:563–581.
- Judson R, Richard A, Dix D, Houck K, Elloumi F, Martin M, et al. ACToR—aggregated computational toxicology resource. *Toxicology and applied pharmacology*. 2008; 233:7–13. [PubMed: 18671997]
- Judson R, Richard A, Dix DJ, Houck K, Martin M, Kavlock R, et al. The toxicity data landscape for environmental chemicals. *Environmental health perspectives*. 2009; 117:685. [PubMed: 19479008]
- Judson RS, Martin MT, Egeghy P, Gangwal S, Reif DM, Kothiya P, et al. Aggregating data for computational toxicology applications: the US Environmental Protection Agency (EPA) aggregated computational toxicology resource (ACToR) system. *International journal of molecular sciences*. 2012; 13:1805–1831. [PubMed: 22408426]
- Kavlock R, Chandler K, Houck K, Hunter S, Judson R, Kleinstreuer N, et al. Update on EPA's ToxCast program: providing high throughput decision support tools for chemical risk management. *Chemical Research in Toxicology*. 2012; 25:1287–1302. [PubMed: 22519603]
- Klamt A, Eckert F, Arlt W. COSMO-RS: an alternative to simulation for calculating thermodynamic properties of liquid mixtures. *Annual review of chemical and biomolecular engineering*. 2010; 1:101–122.



- Klamt A, Eckert F, Diedenhofen M, Beck ME. First Principles Calculations of Aqueous p K a Values for Organic and Inorganic Acids Using COSMO–RS Reveal an Inconsistency in the Slope of the p K a Scale. *The Journal of Physical Chemistry A*. 2003; 107:9380–9386. [PubMed: 26313337]
- Kurebayashi H, Betsui H, Ohno Y. Disposition of a low dose of 14C-bisphenol A in male rats and its main biliary excretion as BPA glucuronide. *Toxicological Sciences*. 2003; 73:17–25. [PubMed: 12700409]
- Kwon Y. *Handbook of essential pharmacokinetics, pharmacodynamics and drug metabolism for industrial scientists* Springer Science & Business Media; 2001
- Lee PH, Ayyampalayam SN, Carreira LA, Shalaeva M, Bhattachar S, Coselmon R, et al. In silico prediction of ionization constants of drugs. *Molecular pharmaceutics*. 2007; 4:498–512. [PubMed: 17629304]
- Liao C, Nicklaus MC. Comparison of nine programs predicting p K a values of pharmaceutical substances. *Journal of chemical information and modeling*. 2009; 49:2801–2812. [PubMed: 19961204]
- Manners CN, Payling DW, Smith DA. Distribution coefficient, a convenient term for the relation of predictable physico-chemical properties to metabolic processes. *Xenobiotica*. 1988; 18:331–350. [PubMed: 3289270]
- Mansouri K, Abdelaziz A, Rybacka A, Roncaglioni A, Tropsha A, Varnek A, et al. CERAPP: Collaborative Estrogen Receptor Activity Prediction Project. *Environ Health Perspect*. 2016
- Mazur CS, Marchitti SA, Dimova M, Kenneke JF, Lumen A, Fisher J. Human and rat ABC transporter efflux of bisphenol a and bisphenol a glucuronide: interspecies comparison and implications for pharmacokinetic assessment. *Toxicological Sciences*. 2012; 128:317–325. [PubMed: 22552776]
- Moscovitz JE, Nahar MS, Shalat SL, Slitt AL, Dolinoy DC, Aleksunes LM. Correlation between Conjugated Bisphenol A Concentrations and Efflux Transporter Expression in Human Fetal Livers. *Drug Metabolism and Disposition*. 2016 dmd. 115.068668.
- Mumtaz M, Fisher J, Blount B, Ruiz P. Application of physiologically based pharmacokinetic models in chemical risk assessment. *Journal of toxicology*. 2012
- National Academies of Sciences E, MedicineUsing 21st Century Science to Improve Risk-Related Evaluations Washington, DC: The National Academies Press; 2017
- Palaz S, Türkkän B, Ero lu E. A QSPR Study for the Prediction of the pKa of N-Base Ligands and Formation Constant Kc of Bis (2, 2'-bipyridine) Platinum (II)-N-Base Adducts Using Quantum Mechanically Derived Descriptors. *ISRN Physical Chemistry*. 2012; 2012
- Pearce RG, Setzer RW, Strope CL, Sipes NS, Wambaugh JF. Httk: R package for high-throughput toxicokinetics. *Journal of Statistical Software*. 2017; 79:1–26.
- Perrin DD, Dempsey B, Serjeant EP. *pKa prediction for organic acids and bases Vol. 1*. Springer; 1981
- Peyret T, Poulin P, Krishnan K. A unified algorithm for predicting partition coefficients for PBPK modeling of drugs and environmental chemicals. *Toxicology and applied pharmacology*. 2010; 249:197–207. [PubMed: 20869379]
- Poulin P, Haddad S. Advancing prediction of tissue distribution and volume of distribution of highly lipophilic compounds from a simplified tissue-composition-based model as a mechanistic animal alternative method. *Journal of pharmaceutical sciences*. 2012; 101:2250–2261. [PubMed: 22388869]
- Poulin P, Krishnan K. A mechanistic algorithm for predicting blood: air partition coefficients of organic chemicals with the consideration of reversible binding in hemoglobin. *Toxicology and applied pharmacology*. 1996a; 136:131–137. [PubMed: 8560466]
- Poulin P, Krishnan K. A tissue composition-based algorithm for predicting tissue: air partition coefficients of organic chemicals. *Toxicology and applied pharmacology*. 1996b; 136:126–130. [PubMed: 8560465]
- Poulin P, Theil FP. A priori prediction of tissue: plasma partition coefficients of drugs to facilitate the use of physiologically-based pharmacokinetic models in drug discovery. *Journal of pharmaceutical sciences*. 2000; 89:16–35. [PubMed: 10664535]

- Richard AM, Williams CR. Distributed structure-searchable toxicity (DSSTox) public database network: a proposal. *Mutation Research/Fundamental and Molecular Mechanisms of Mutagenesis*. 2002; 499:27–52. [PubMed: 11804603]
- Rodgers T, Leahy D, Rowland M. Physiologically based pharmacokinetic modeling 1: predicting the tissue distribution of moderate-to-strong bases. *Journal of pharmaceutical sciences*. 2005; 94:1259–1276. [PubMed: 15858854]
- Rodgers T, Rowland M. Physiologically based pharmacokinetic modelling 2: predicting the tissue distribution of acids, very weak bases, neutrals and zwitterions. *Journal of pharmaceutical sciences*. 2006; 95:1238–1257. [PubMed: 16639716]
- Schmitt W. General approach for the calculation of tissue to plasma partition coefficients. *Toxicology in Vitro*. 2008; 22:457–467. [PubMed: 17981004]
- ADMET Predictor 2017 Simulations Plus.
- Smith DA, Beaumont K, Maurer TS, Di L. Volume of Distribution in Drug Design: Miniperspective. *Journal of medicinal chemistry*. 2015; 58:5691–5698. [PubMed: 25799158]
- Szegezdi J, Cszimadia F. Calculating pKa values of small and large molecules. 233rd ACS National Meeting; Chicago, IL. 2007;
- Szegezdi J, Cszimadia F. Prediction of dissociation constant using microconstants. 227th ACS National Meeting; Anaheim, California. 2004;
- Teegarden JG, Waechter JM, Clewell HJ, Covington TR, Barton HA. Evaluation of oral and intravenous route pharmacokinetics, plasma protein binding, and uterine tissue dose metrics of bisphenol A: a physiologically based pharmacokinetic approach. *Toxicological Sciences*. 2005; 85:823–838. [PubMed: 15746009]
- Thomas RS, Philbert MA, Auerbach SS, Wetmore BA, Devito MJ, Cote I, et al. Incorporating new technologies into toxicity testing and risk assessment: moving from 21st century vision to a data-driven framework. *Toxicol Sci*. 2013; 136:4–18. [PubMed: 23958734]
- Tice RR, Austin CP, Kavlock RJ, Bucher JR. Improving the human hazard characterization of chemicals: a Tox21 update. *Environmental Health Perspectives*. 2013; 121:756. [PubMed: 23603828]
- Tukey JW. *Exploratory data analysis* 1977
- USEPA/EPI (Estimation Programs Interface) Suite 2015
- USGAAOffice GAC hemical Regulation: Options for Enhancing the Effectiveness of the Toxic Substances Control Act 2009
- USGAAOffice USGAToxic Substances: EPA Has Increased Efforts to Assess and Control Chemicals but Could Strengthen Its Approach 2013
- Vareková RS, Geidl S, Ionescu C-M, Skrehota O, Kudera M, Sehnal D, et al. Predicting pKa Values of Substituted Phenols from Atomic Charges: Comparison of Different Quantum Mechanical Methods and Charge Distribution Schemes. *Journal of chemical information and modeling*. 2011; 51:1795–1806. [PubMed: 21761919]
- Weininger D. SMILES, a chemical language and information system. 1. Introduction to methodology and encoding rules. *Journal of chemical information and computer sciences*. 1988; 28:31–36.
- Wetmore BA, Wambaugh JF, Allen B, Ferguson SS, Sochaski MA, Setzer RW, et al. Incorporating High-Throughput Exposure Predictions With Dosimetry-Adjusted In Vitro Bioactivity to Inform Chemical Toxicity Testing. *Toxicological Sciences*. 2015; 148:121–36. [PubMed: 26251325]
- Wetmore BA, Wambaugh JF, Ferguson SS, Sochaski MA, Rotroff DM, Freeman K, et al. Integration of dosimetry, exposure, and high-throughput screening data in chemical toxicity assessment. *Toxicological Sciences*. 2012; 125:157–74. [PubMed: 21948869]
- Wilson MP, Schwarzman MR. Toward a new U.S. chemicals policy: rebuilding the foundation to advance new science, green chemistry, and environmental health. *Environ Health Perspect*. 2009; 117:1202–9. [PubMed: 19672398]
- Xing L, Glen RC, Clark RD. Predicting p K a by molecular tree structured fingerprints and PLS. *Journal of chemical information and computer sciences*. 2003; 43:870–879. [PubMed: 12767145]
- Yoo SD, Shin BS, Kwack SJ, Lee BM, Park KL, Han S-Y, et al. Pharmacokinetic disposition and tissue distribution of bisphenol A in rats after intravenous administration. *Journal of toxicology and environmental health Part A*. 2000; 61:131–139. [PubMed: 11032426]

Yoon M, Campbell JL, Andersen ME, Clewell HJ. Quantitative in vitro to in vivo extrapolation of cell-based toxicity assay results. *Critical reviews in toxicology*. 2012; 42:633–652. [PubMed: 22667820]

## Appendix

Several  $pK_a$  prediction programs exist (Liao and Nicklaus, 2009). Commercial predictors span a range of mechanisms to predict the protonation state of particular atoms, including linear free energy relationships (LFER) that use a dictionary of chemical substructures (Lee et al., 2007), quantitative structure-property relationships (QSPR) (Jover et al., 2008; Palaz et al., 2012), and quantum chemical and *ab initio* methods (Bochevarov et al., 2013; Eckert and Klamt, 2006; Eckert et al., 2009; Klamt et al., 2010; Klamt et al., 2003; Vareková et al., 2011). Semi-empirical models calculate descriptors for each ionizable chemical functional group, after which  $pK_a$  values are predicted using machine learning or tree-based models (Jelfs et al., 2007; Xing et al., 2003). These semi-empirical models are limited by the number of chemicals used (Xing et al., 2003) and the usage of a proprietary, non-releasable training set (Jelfs et al., 2007).

Empirical methods employ substructure databases and use LFER to predict  $pK_a$  values based on the prior assignments for the atomic groups stored in a database. As such, their prediction accuracy is limited to the substructures contained in their database. If additional training data are available, many of these tools can be recalibrated to apply to new chemical structures. Unfortunately, such data are not available for many environmental chemicals. The data limitations of these methods will improve with the addition of more  $pK_a$  data and could be aided by efforts to contribute  $pK_a$  data that are currently underway (<https://gist.github.com/egonw/5aa53abe480a8625fe81>). Such is also the case with predictors using QSPR. These prediction methods have been developed using machine learning algorithms along with structural and chemical descriptors to make predictions of  $pK_a$  values (Fraczkiewicz et al., 2014; Szegezdi and Csizmadia, 2007; Szegezdi and Czismadia, 2004).

Quantum chemical methods and *ab initio* methods offer great promise, but currently both are computationally intensive and generally do not perform as well as LFER and QSPR methods (Elyashberg et al., 2010). Due to their computational inefficiency, these methods are incompatible with high-throughput methodologies.

The majority of  $pK_a$  prediction programs inspect a particular chemical, including the interplay between ionizable sites, to predict the  $pK_a$  value. Calculating the interactions between sites, however, exponentially increases the computation time. In SPARC (Lee et al., 2007), chemicals with complex atomic interactions can result in calculations that last weeks to months for a single chemical, for which SPARC will return an incomplete calculation error (Lee et al., 2007).

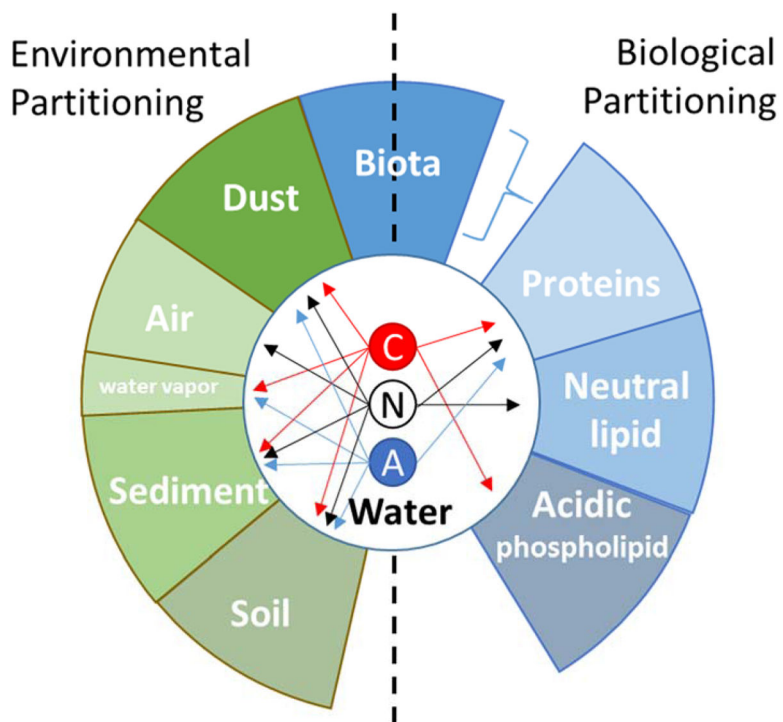


**Fig. 1.** Neutral and ionized species of the same molecule can partition differently into environmental and biological media (C = cation, N = neutral, and A = anion). Ecologically only neutral species partition into air, while only ions partition onto water droplets (Franco and Trapp, 2008); all species can partition into dust, sediment, and soil (Doucette, 2003; Franco et al., 2009). Biologically both neutral and ionized forms can bind to proteins, while cations can partition into acidic phospholipids and neutral species can partition into neutral lipids (Peyret et al., 2010).

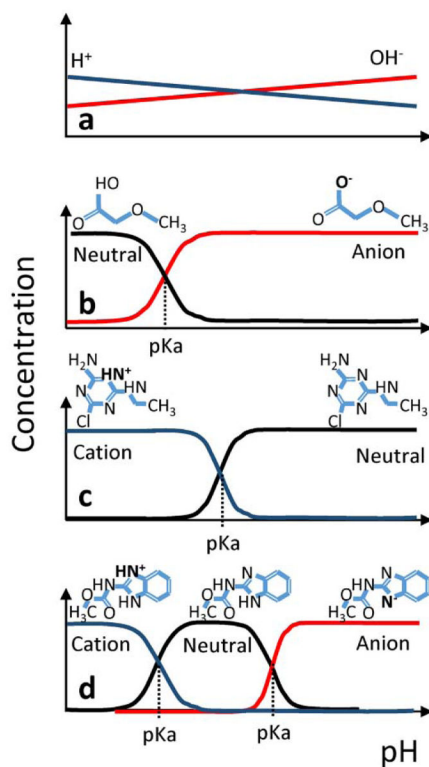


**Fig. 2.**

The scalar  $pK_a$  characterizes the pH at which two chemical microspecies are in equilibrium, as a function of the concentration of hydrogen cations and hydroxide anions (panel a). The relative concentrations of ionized and neutral species depend not only on the  $pK_a$ , but on the number of hydrogen donor groups (panel b), hydrogen acceptor groups (panel c), or a combination of both groups (panel d). Since multiple donor/acceptor groups can occur in a single molecule, the group(s) on the molecule becoming ionized must be identified.

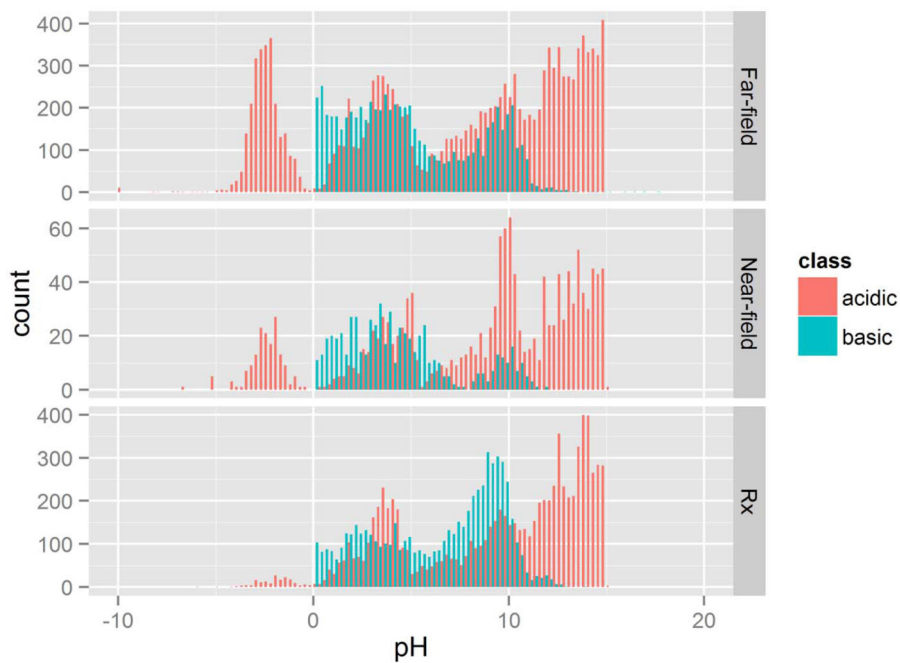


**Fig. 3.** Profile of the number of association and dissociation actions of predicted ionization sites with  $pK_a$  values from ChemAxon versus the pH at which the ionization occurs. Note that  $pK_a$  predictions are calculated at 25°C; at physiological temperatures, 37°C, will generally shift predictions slightly to the left (towards pH 0) (Perrin et al., 1981).

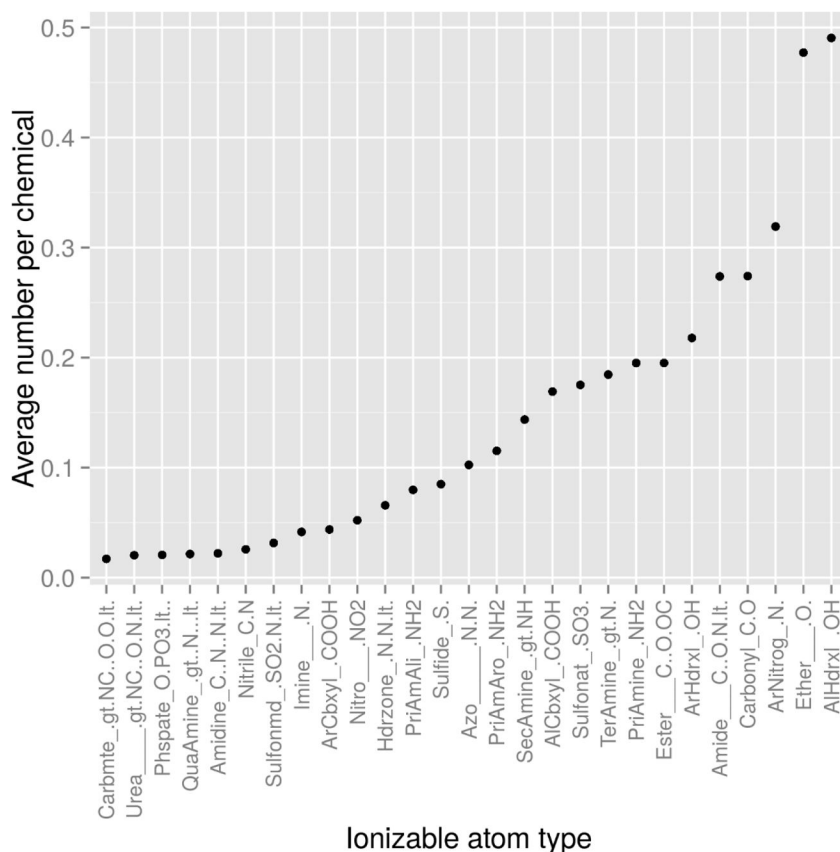


**Fig. 4.** Average number of occurrences per chemical for a subset of IATs, normalized by the total number of chemicals in each class. IATs considered in this work are the non-terminally charged subset of IATs with more than 0.1 IAT per chemical.

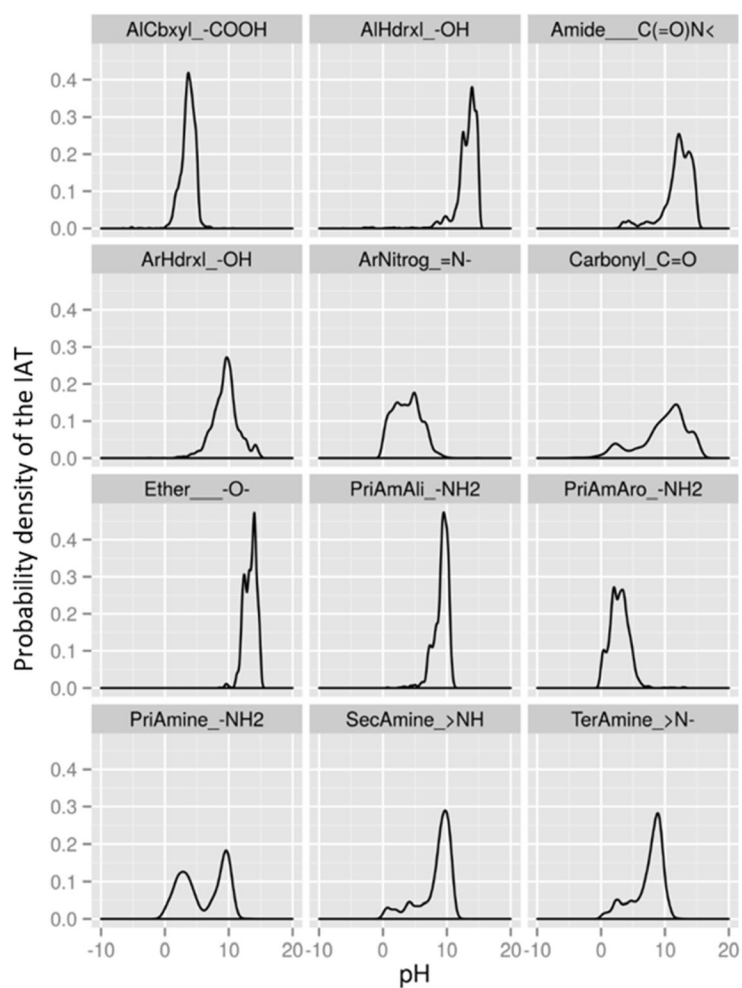


**Fig. 5.** Probability density of pKa for IATs predicted from the 32413 chemicals using ChemAxon pKa Plugin for selected IATs from Fig. 4.



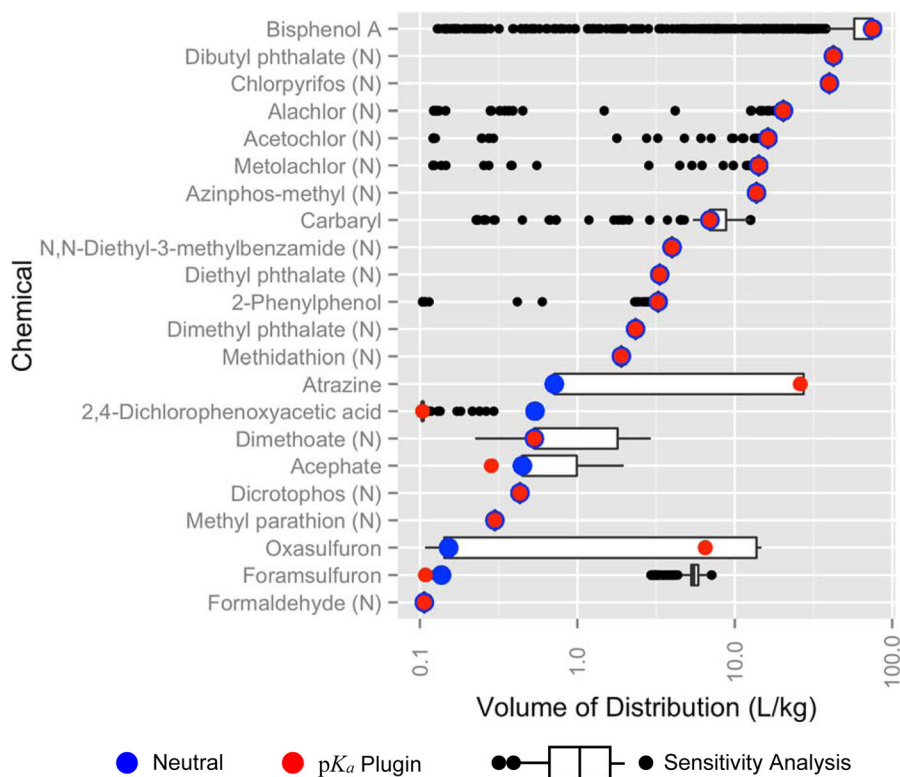


**Fig. 6.** Apparent  $V_{d_{ss}}$  calculated for each chemical based on 2000 samples with replacement from the IAT probability distributions shown in Fig 5. Non-ionizable chemicals are denoted with (N). Box and whiskers plot shows the predicted  $pK_a$  values, with black dots indicating outliers beyond 1.5 x interquartile range. The assumption that no IATs are ionized is shown in blue, and the chemical apparent  $V_{d_{ss}}$  values using  $pK_a$  plugin predictions are shown in red.

**Table 1**

General framework of chemical classification determined by chemical exposure potential and expectation of biological activity.

<b>Chemical Type</b>	<b>Human Exposure Scenario</b>
Pharmaceutical	Compounds intended to be taken as a dose to cause bioactivity.
Near-field environmental	Compounds with proximate sources of exposure that might lead to higher doses, but are not intended to cause bioactivity.
Far-field environmental	Compounds with distal sources of exposure that should lead to lower doses, but bioactivity restrictions are less constrained.

Table 2

NHANES chemicals with corresponding IAT,  $F_u$  reported in (Wetmore et al., 2015; Wetmore et al., 2012), and  $Vd_{ss}$  calculated using  $pK_{a,s}$  predicted by pKa Plugin Neutral chemicals are included at the bottom.

Compound	logP	Ionizable Atom Type	$pK_a$	$F_u$	$Vd_{ss}$
Oxasulfuron	1.13	ArNitrog= $N^-$	2.33	0.061	6.498
		Amide__C(=O)N<	3.5		
Foramsulfuron	0.59	SecAmine_ $\rightarrow$ NH	3.46	0.065	0.108
Carbaryl	2.46	Amide__C(=O)N<	14.77	0.692	6.708
Bisphenol A (BPA)	4.04	ArHdxl_ $-OH$	9.78	0.257	74.228
		ArHdxl_ $-OH$	10.39		
Atrazine	2.20	SecAmine_ $\rightarrow$ NH	14.62	0.112	25.899
		ArNitrog= $N^-$	3.2		
Acephate	-0.33	SecAmine_ $\rightarrow$ NH	6.54	0.868	0.283
2-Phenylphenol	3.32	ArHdxl_ $-OH$	9.69	0.041	3.137
2,4-Dichlorophenoxyacetic acid	2.5	AlCbxy_ $-COOH$	2.81	0.040	0.104
Neutral Chemicals					
Azinphos-methyl	3.24			0.214	13.286
Chlorpyrifos	4.78			0.018	39.176
Dimethoate	0.34			0.965	0.528
Methidathion	2.29			0.268	1.834
Methyl parathion	2.60			0.014	0.292
Diethyl phthalate	2.69			0.190	3.221
Dibutyl phthalate	4.63			0.028	41.594
Dimethyl phthalate	1.98			0.656	2.264
N,N-Diethyl-3-methylbenzamide	2.50			0.356	3.855
Dicrotophos	-0.24			0.823	0.429
Alachlor	3.59			0.141	19.740
Metolachlor	3.45			0.133	13.756
Formaldehyde	-0.47			1	0.107
Acetochlor	3.50			0.135	15.735

With this data, the focus of this sensitivity analysis was the body burden of each compound, derived through the prediction of PK distribution of a chemical within the body.

EPA Author Manuscript

EPA Author Manuscript

EPA Author Manuscript

**Table 3**

Fraction of times each IAT pattern is ionized in pK<sub>a</sub> plug-in predictions versus the total number identified in the SMILES string.

IAT	Ionized/Total	%	IAT	Ionized/Total	%	IAT	Ionized/Total	%
AlCbxyL-COOH	3336/3427	97%	AlHdxL-OH	4267/9971	43%	Amide__C(=O)N<	2262/5992	38%
ArHdxL-OH	3110/4287	73%	ArNitrog_=N-	2845/6884	41%	Carbonyl_C=O	507/7518	7%
Ether____-O-	1352/13394	10%	PriAmAli_-NH2	1230/1341	92%	PriAmAro_-NH2	1240/2308	54%
PriAmine_-NH2	2469/3649	68%	SecAmine_>NH	1031/2898	36%	TerAmine_>N-	3144/4539	69%